

Article

G-Quadruplex DNzyme Molecular Beacon for Amplified Colorimetric Biosensing of *Pseudostellaria heterophylla*

Zhenzhu Zheng¹, Jing Han¹, Wensheng Pang^{2,3} and Juan Hu^{1,2,*}

¹ Institute of Drug Research, Fujian Academy of Chinese Medicine, Fuzhou 350003, China; E-Mails: smilepearl727@gmail.com (Z.Z.); drjinghan@gmail.com (J.H.)

² The College of Pharmacy, Fujian University of Traditional Chinese Medicine, Fuzhou 350122, China; E-Mail: pws@fjtc.edu.cn (W.P.)

³ The Second People's Hospital of Fujian Province, Fuzhou 350003, China

* Author to whom correspondence should be addressed; E-Mail: huj@fjtc.edu.cn; Tel./Fax: +86-591-8357-0397.

Received: 12 December 2012; in revised form: 4 January 2013 / Accepted: 9 January 2013 /

Published: 16 January 2013

Abstract: With an internal transcribed spacer of 18 S, 5.8 S and 26 S nuclear ribosomal DNA (nrDNA ITS) as DNA marker, we report a colorimetric approach for authentication of *Pseudostellaria heterophylla* (PH) and its counterfeit species based on the differentiation of the nrDNA ITS sequence. The assay possesses an unlabelled G-quadruplex DNzyme molecular beacon (MB) probe, employing complementary sequence as biorecognition element and 1:1:1:1 split G-quadruplex halves as reporter. In the absence of target DNA (T-DNA), the probe can shape intermolecular G-quadruplex structures capable of binding hemin to form G-quadruplex-hemin DNzyme and catalyze the oxidation of ABTS²⁻ to blue-green ABTS^{•-} by H₂O₂. In the presence of T-DNA, T-DNA can hybridize with the complementary sequence to form a duplex structure, hindering the formation of the G-quadruplex structure and resulting in the loss of the catalytic activity. Consequently, a UV-Vis absorption signal decrease is observed in the ABTS²⁻-H₂O₂ system. The “turn-off” assay allows the detection of T-DNA from 1.0×10^{-9} to 3.0×10^{-7} mol L⁻¹ ($R^2 = 0.9906$), with a low detection limit of 3.1×10^{-10} mol L⁻¹. The present study provides a sensitive and selective method and may serve as a foundation of utilizing the DNzyme MB sensor for identifying traditional Chinese medicines.

Keywords: G-quadruplex DNAzyme; molecular beacon; colorimetric; *Pseudostellaria heterophylla*

1. Introduction

Pseudostellaria heterophylla (PH), a common traditional Chinese medicine, has been utilized to treat night sweats, hyperirritability, asthenia after illnesses, various lung and spleen diseases [1–4]. However, many counterfeit species, e.g., *Lophatherum gracile* (LG), *Liriope platyphylla* (LP), *Ophiopogon japonicus* (OJ), *Stemona sessilifolia* (SS) and *Stemona japonica* (SJ) [5], are misused in the market owing to their lower cost or erroneous identification. The counterfeit species may have weaker or completely different pharmacological actions compared with the authentic counterpart, and thus the authentication is the key to ensure the therapeutic effect and raise consumers' confidence in Traditional Chinese Medicine [6]. Nowadays, analysis of well-characterized marker compounds is the most popular method for identifying the herbal species utilizing HPLC [7,8], HPCE [9], GC-MS [10,11], NIR spectroscopy [4], etc. However, in many herbal medicines the chemical compounds change with external environment and processing conditions, which diminishes the reliability of these identification methods. Genetic composition is unique for each individual herbal species and is less influenced by environmental and processing factors. As reported, internal transcribed spacer of 18S, 5.8S and 26S nuclear ribosomal DNA (nrDNA ITS) has proven to be a particularly valuable resource for phylogenetic analysis in many angiosperm families [12–16]. Nowadays, many genetic tools have been utilized for the authentication of herbal species, e.g., RAPD [17], RFLP [18], MASA [18], MAS-PCR [19]. The practicality of these methods varies with their sensitivity, reliability and cost of execution [20]. Hence, the development of a sensitive, reliable and low-cost analytical method based on DNA sequences is desirable. G-quadruplex molecular beacon (MB) DNAzyme, a label-free and amplified detecting assay, fulfills all these requirements.

Since their discovery in 1996 [21], molecular beacons (MBs) have been extensively utilized in biological applications [22,23]. MBs are initially designed with a hairpin shape, featuring a stem-loop structure [21,24]. While the stem part is usually built with Watson-Crick hydrogen bonding between natural DNA base pairs, the 5'- and 3'-ends of a MB structure are labeled with a fluorophore and a quencher, respectively [25,26]. However, the employment of the fluorophore and quencher results not only in high costs, but also complexity of processes [26].

G-quadruplex DNAzyme, formed by the folding of four G-rich repeats and binding with hemin, possesses a property mimicking horseradish peroxidase (HRP) [27–30] and catalyzes the H₂O₂-mediated oxidation of the colorless 2,2'-azino-bis(3-ethylbenzthiazoline-6-sulfonic acid) diammonium salt (ABTS²⁻) into the blue-green radical anion ABTS^{•-} [31–34] to achieve signal amplification in DNA detection [35]. Moreover, the unusual G-rich nucleic acid has been found to possibly split the whole sequence [33,36] and lead to an extraordinary selectivity for the detection of nucleic acids [37], proteins and other biomolecules [31,38]. Also, the utilization of split G-quadruplex makes the assay design more flexible [39].

Wang and co-workers have employed a split G-quadruplex DNzyme tethered to both the ends as reporter instead of the fluorophore/quencher combination, which avoids any complex labeling process [26]. Considering these advantages, we have also combined the split G-quadruplex structure and MB technique to develop a label-free G-quadruplex DNzyme MB oligonucleotide sensor for biosensing of PH nrDNA ITS sequences. In the sensor, a novel 1:1:1:1 split mode of G-quadruplex is utilized and one GGG repeat is tethered to both the ends as the reporter. The complementary sequence for target PH nrDNA ITS sequence locates at the loop portion and serves as sensing element.

2. Experimental

2.1. Materials

All the oligonucleotides were first synthesized and purified by Sangon Biotechnology Co., Ltd. (Shanghai, China). The working solutions (10^{-4} mol L⁻¹) of oligonucleotides were prepared in 25 mM Tris-HAc buffer (pH 7.0) and stored at 4 °C until used. Hemin was purchased from Aladdin Reagents (Shanghai, China) and the stock solution was prepared in dimethyl sulfoxide (DMSO). H₂O₂ was purchased from Fuchen Chemical Reagents (Tianjin, China) and ABTS was purchased from Aladdin Reagents. Before used, H₂O₂, ABTS, and hemin working solutions were prepared in working buffer (pH 7.5) containing 50 mM Tris-HCl, 150 mM NH₄Cl, 20 mM KCl, 0.03% Triton X-100 and 1% DMSO. All reagents were used as received without further purification.

2.2. Instrumentation

A Perkin Elmer (Lambda 750) UV-vis-NIR spectrophotometer was used to collect the UV-vis absorbance spectra of the ABTS²⁻-H₂O₂ reaction system. Circular dichroism (CD) experiments were performed on an Aviv Model 420 spectrometer (Aviv, Lakewood, NJ, USA).

2.3. Assay Procedure

In a typical assay, 0.5 µL of probe (5.0×10^{-5} mol L⁻¹) was hybridized with different concentrations of T-DNA in Tris-HOAc buffer (25 mM) for 40 min at room temperature. After that, 0.8 µL of hemin solution (6.25×10^{-5} mol L⁻¹) was added and the mixture was incubated for 60 min. Then, 20 µL of ABTS (2.5×10^{-2} mol L⁻¹), 2.5 µL of H₂O₂ (0.2 mol L⁻¹), and the working buffer (50 mM Tris-HCl, pH 7.5, 150 mM NH₄Cl, 20 mM KCl, 0.03% Triton X-100 and 1% DMSO) were added to adjust the volume to 250 µL. After 5 min, the UV-vis spectrum was collected on a Perkin Elmer UV-vis-NIR spectrophotometer at room temperature and the photo was taken immediately. The maximum absorption wavelength of the oxidation product ABTS^{•-} was about 419 nm.

2.4. CD Measurements

In the circular dichroism (CD) experiments, 2.5 µL of probe-1, probe-2, probe-3, probe-4 (1.0×10^{-4} mol L⁻¹) in the absence of T-DNA were respectively added to 247.5 µL of working buffer (50 mM Tris-HCl, pH 7.5, 150 mM NH₄Cl, 20 mM KCl, 0.03% Triton X-100 and 1% DMSO) and incubated for 60 min. In the T-DNA-containing system, 2.5 µL of probe-4 (1.0×10^{-4} mol L⁻¹) and

2.5 μL of T-DNA ($1.0 \times 10^{-4} \text{ mol L}^{-1}$) were first mixed together and incubated for 40 min. After that, 245 μL of the working buffer was added to the mixture and then also incubated for 60 min. Finally, the CD spectra were measured on an Aviv Model 420 spectrometer at room temperature. The wavelengths were scanned from 220 to 320 nm, with a step of 2 nm and bandwidth of 1 nm.

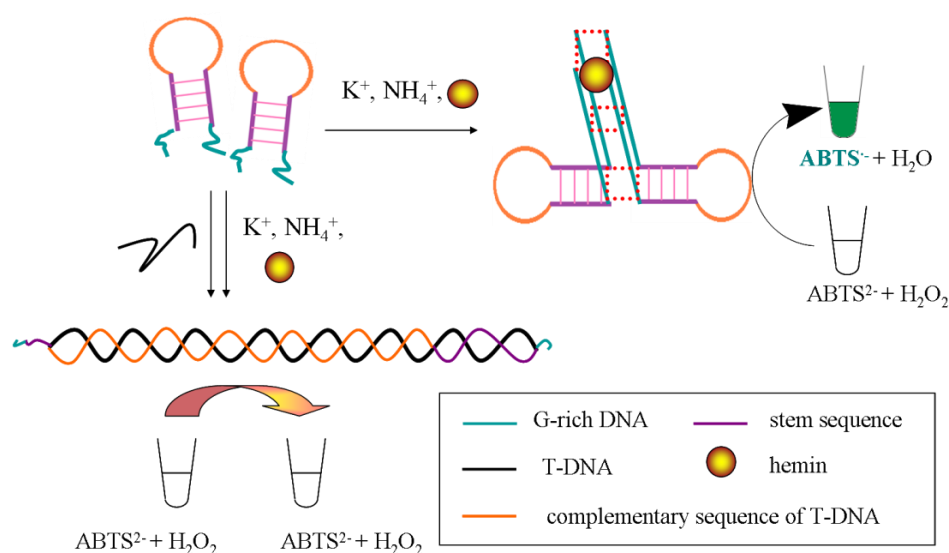
3. Results and Discussion

3.1. Principle of the DNAzyme MB Sensor Detecting PH nrDNA ITS Sequence

According to the differentiation between PH and its counterfeit species in nrDNA ITS sequence, a section of the nrDNA ITS sequence specific for PH works as target and is labeled as T-DNA. The nrDNA ITS sequences specific for the counterfeit species are labeled as C-DNA.

As shown in Figure 1, the complementary sequence for T-DNA locates at the hairpin loop and serves as the sensing element. In the absence of T-DNA, two oligonucleotide probes shape an intermolecular G-quadruplex structure through the association of the GGG repeats. Then hemin is able to specifically bind to the G-quadruplex with high affinity and yield a DNAzyme which can catalyze the oxidation of ABTS^{2-} by H_2O_2 to the colored product $\text{ABTS}^{\cdot-}$ revealed by a strong UV-vis absorption signal. In the presence of T-DNA, the loop of the MB sensor is combined and the stem opens to form a duplex DNA structure hindering the formation of the intermolecular G-quadruplex DNAzyme and leading to the loss of the catalytic activity. As a result, a weaker UV-vis absorption signal can be observed in the ABTS^{2-} - H_2O_2 reaction system.

Figure 1. Working principle of the 1:1:1:1 split G-quadruplex DNAzyme MB sensor for PH nrDNA ITS.



3.2. Design of Probes

In this work, four types of probe were designed. Probe-1 was designed with the middle sequence (orange characters) complementary to T-DNA and both ends possessing two GGG repeats (green characters) according to the frequently used 2:2 split mode. Furthermore, an insertion of seven nucleotides (violet characters) for hairpin stem structure was applied in probe-2. Probe-3 was designed

with the middle sequence (orange characters) complementary to T-DNA and one GGG repeat (green characters) locating at both ends according to the fresh 1:1:1:1 split mode. Then probe-4 was designed by further inserting seven nucleotides (violet characters). All the oligonucleotides were listed in Table 1.

Table 1. Sequences of the oligonucleotides used in the assembly of the G-quadruplex DNAzyme MB sensor.

Oligomer		Sequence (from 5' to 3')
T-DNA	PH	TCGAAACCTG CCCAGC - - - AGAACGACCA GCGAACA
C-DNA	LG	TCG TGACCCT T - - AAC - - - AA AACAGACC GCGCACG
	LP	TCAACACGTG TGCAGTTTAG AGCATACT CA ATA AACA
	OJ	TCAATACGTG TG - AGTTTA - AGCATACTCA ATA AACA
	SS	TCAATACATG TGCAGTTTA - AG CATACTCA GTGAACA
	SJ	TCAGTACATG TGCAGTTTAG AGCATA -TCA ATA AACA
	probe	probe-1
probe-2		GGGATT GGGATT TGTTTCGC TGGTCGTTCTGCTGGGCAGGTTTCGA GCGAACA TTAGGG TTAGGG
probe-3		GGGATT TGTTTCGCTGGTCGTTCTGCTGGGCAGGTTTCGA TTAGGG
probe-4		GGGATT TGTTTCGC TGGTCGTTCTGCTGGGCAGGTTTCGA GCGAACA TTAGGG
Hum24		(TTAGGG) ₄

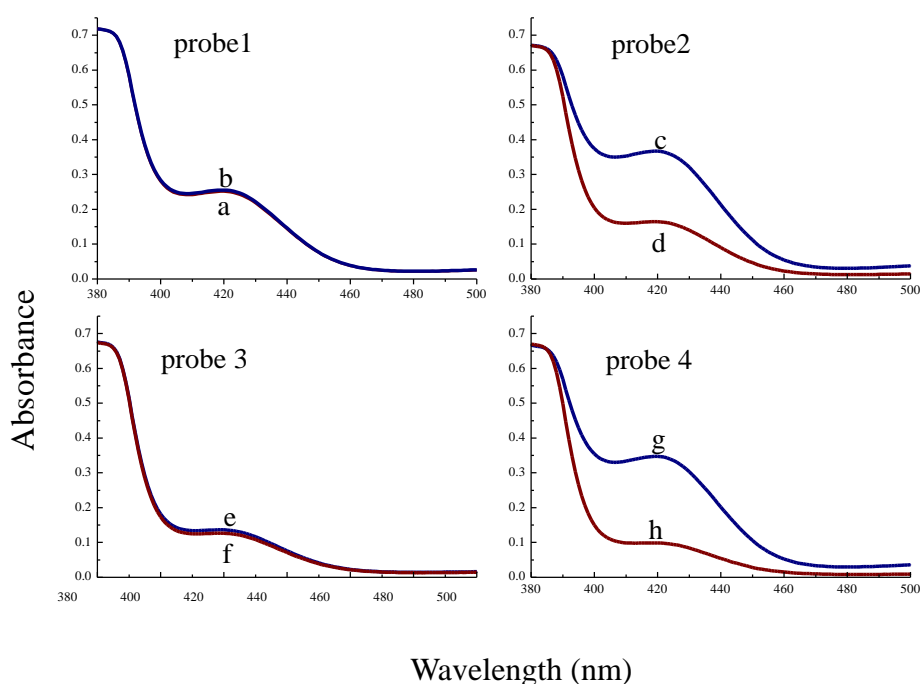
3.3. Optimization of Probe

As introduced in Section 3.2, probe-1 and probe-2 were designed with 2:2 G-quadruplex split mode while probe-3 and probe-4 were designed with 1:1:1:1 split mode. Probe-2 and probe-4 had a loop-stem structure by inserting seven nucleotides while probe-1 and probe-3 did not. To obtain an optimum oligonucleotide probe, the catalytic activity of the four probes was investigated and compared under the same conditions. Figure 2 shows that the UV-vis absorbance spectrum of the probe-1 system has nearly no change induced by T-DNA while a decreasing rate of 223% induced by T-DNA is observed in the probe-2 system.

Meanwhile, the absorbance signal of the probe-3 system decreases a little, and a rate of decrease of 351% induced by T-DNA is observed in the probe-4 system. From the results, we can find that the probe-3 system and probe-4 system have larger decrease rates than the probe-1 and probe-2 systems, respectively. This is because while binding with T-DNA both probe-1 and probe-2 with 2:2 split mode could still assemble to form the G-quadruplex structure more easily than probe-3 and probe-4, respectively, and the middle G-quadruplex DNAzyme is less disrupted. Therefore, the probes with 2:2 split mode have stronger background signals.

Meanwhile, the probe-2 system and probe-4 system both possessing hairpin structure have larger decrease rates than the probe-1 system and probe-3 system, respectively. That may be because the stem part of a hairpin structure promotes the probes into shaping G-quadruplex structures and makes the G-quadruplex structure more difficult to dissociate in the absence of T-DNA. As a result, probe-4 with 1:1:1:1 split mode and hairpin structure is chosen as the optimum probe in the whole experiment.

Figure 2. Absorbance spectra of the H_2O_2 mediated ABTS^{2-} colorimetric system. (a) probe-1 ($1.0 \times 10^{-7} \text{ mol L}^{-1}$); (b) probe-1 ($1.0 \times 10^{-7} \text{ mol L}^{-1}$), T-DNA ($1.0 \times 10^{-7} \text{ mol L}^{-1}$); (c) probe-2 ($1.0 \times 10^{-7} \text{ mol L}^{-1}$); (d) probe-2 ($1.0 \times 10^{-7} \text{ mol L}^{-1}$), T-DNA ($1.0 \times 10^{-7} \text{ mol L}^{-1}$); (e) probe-3 ($1.0 \times 10^{-7} \text{ mol L}^{-1}$); (f) probe-3 ($1.0 \times 10^{-7} \text{ mol L}^{-1}$), T-DNA ($1.0 \times 10^{-7} \text{ mol L}^{-1}$); (g) probe-4 ($1.0 \times 10^{-7} \text{ mol L}^{-1}$); (h) probe-4 ($1.0 \times 10^{-7} \text{ mol L}^{-1}$), T-DNA ($1.0 \times 10^{-7} \text{ mol L}^{-1}$).

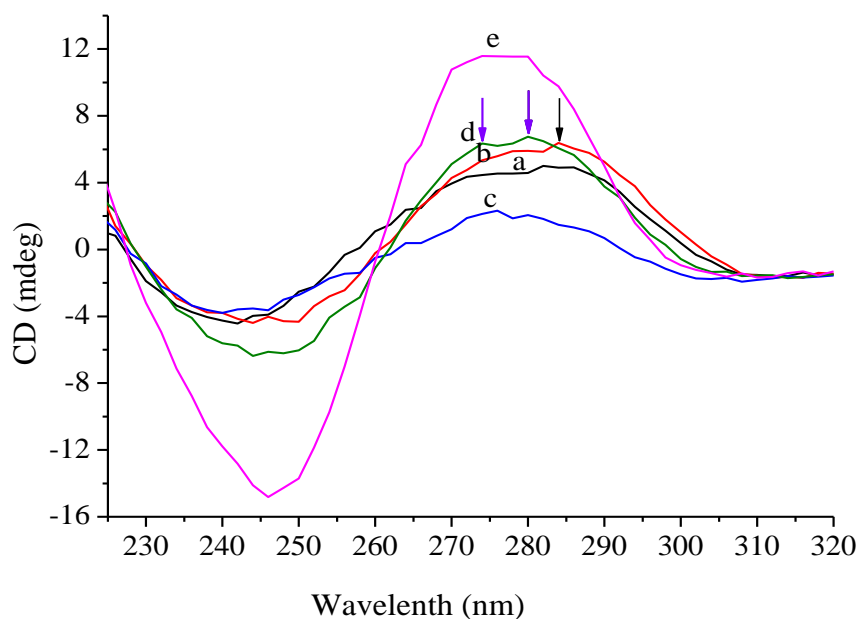


3.4. CD Spectra of Probes

It has been reported that CD spectrum of a typical parallel G-quadruplex structure has a positive peak at 265 nm and a negative band near 240 nm, and that of a typical antiparallel G-quadruplex structure shows a positive peak near 295 nm and a negative peak close to 265 nm [40], while that of a B form duplex DNA structure has a positive peak at 277 nm and a negative peak at 245 nm [41]. To demonstrate the secondary structure shapes in the four probes, CD spectra of the probes were measured in the presence or absence of T-DNA.

From the spectra in Figure 3, we can find that all the probe systems have a negative band around 245 nm, and there is some shift in the positive band. Probe-1 (line a) exhibits a positive peak at around 282 nm, probe-2 (line b) at 284 nm and a shoulder peak at around 274 nm, probe-3 (line c) at around 276 nm, and probe-4 (line d) has a positive peak at 280 nm and a shoulder peak at around 274 nm. The results indicate that all four probes have the ability of shaping a G-quadruplex structure. The weakest CD signal of probe-3 system suggests the least G-quadruplex shape. Furthermore, the engineered stem part induces probe-2 and probe-4 to show a shoulder peak at 274 nm. In the presence of T-DNA, the CD spectrum of probe-4 exhibits a larger positive peak around 277 nm, suggesting the existence of a B form duplex DNA structure. This may be due to the principle that the added T-DNA combines the loop section of probe-4 to form a duplex structure.

Figure 3. CD spectra of (a) probe-1 ($1.0 \times 10^{-6} \text{ mol L}^{-1}$), (b) probe-2 ($1.0 \times 10^{-6} \text{ mol L}^{-1}$), (c) probe-3 ($1.0 \times 10^{-6} \text{ mol L}^{-1}$), (d) probe-4 ($1.0 \times 10^{-6} \text{ mol L}^{-1}$), (e) probe-4 ($1.0 \times 10^{-6} \text{ mol L}^{-1}$) + T-DNA ($1.0 \times 10^{-6} \text{ mol L}^{-1}$).

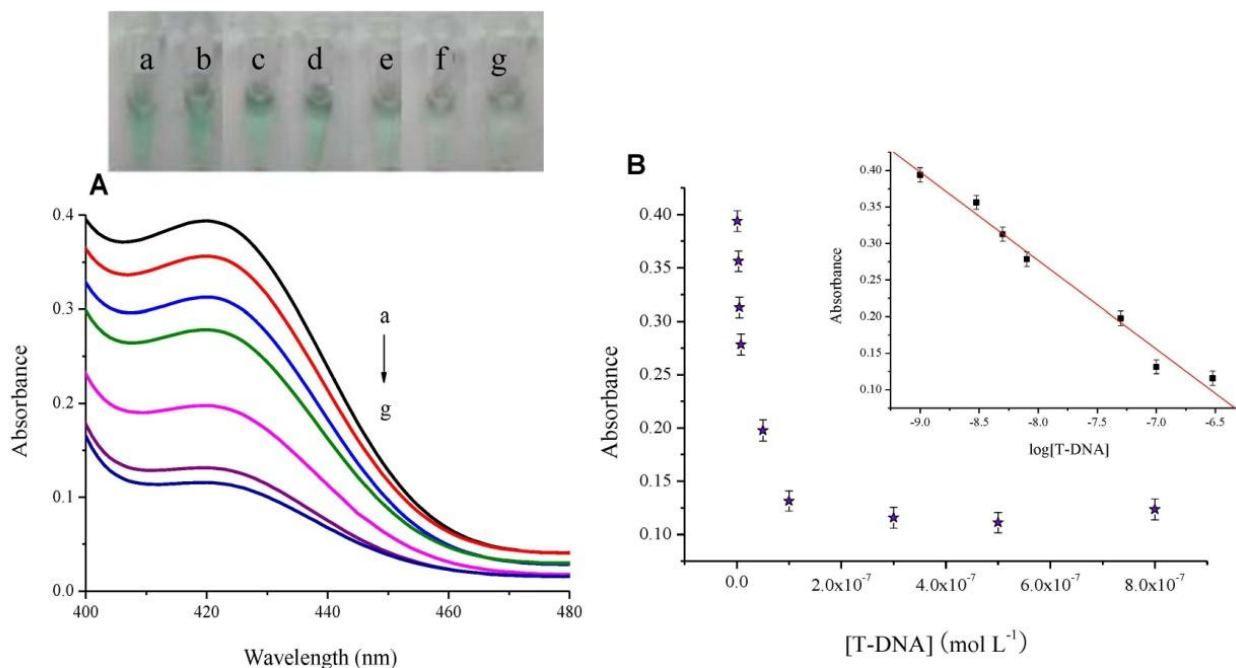


3.5. Colorimetric Analysis of T-DNA

According to the general procedure mentioned in Section 2.3, we have utilized the biofunctional probe-4 to analyze different concentrations of T-DNA in the range of 1.0×10^{-9} to $8.0 \times 10^{-7} \text{ mol L}^{-1}$ by collecting the absorbance spectra and colorimetric signals of the colored product $\text{ABTS}^{\cdot-}$. As shown in Figure 4(A), in the presence of $1.0 \times 10^{-9} \text{ mol L}^{-1}$ T-DNA, the $\text{ABTS}^{2-}\text{-H}_2\text{O}_2$ reaction system promoted by the G-quadruplex DNzyme MB probe shows a strong absorbance and colorimetric signal (curve a, picture a). As the increase of T-DNA concentration, UV-vis absorbance (curve b to g) and colorimetric signal (picture b to g) both decrease gradually. The above results indicate that in the presence of T-DNA, T-DNA hybridizes with the loop part to form a duplex structure and blocks the formation of the middle intermolecular G-quadruplex DNzyme, resulting in a loss of catalytic activity.

As shown in Figure 4(B), the maximal absorbance value at 419 nm decreases obviously with an increasing concentration of T-DNA and then levels off after $3.0 \times 10^{-7} \text{ mol L}^{-1}$. Additionally, the inset is the calibration curve for quantitative analysis. It shows that the absorbance is linearly dependent on the logarithm of T-DNA concentration in the range from 1.0×10^{-9} to $3.0 \times 10^{-7} \text{ mol L}^{-1}$ ($R^2 = 0.9906$). Furthermore, the average absorbance values for the blank systems ($n = 8$) are tested to be 0.3804 (RSD = 4.79%). The detection limit ($3\sigma/\text{slope}$) is estimated to be $3.1 \times 10^{-10} \text{ mol L}^{-1}$. The results indicate that the G-quadruplex DNzyme MB sensor can be a sensitive oligonucleotide assay for identifying T-DNA.

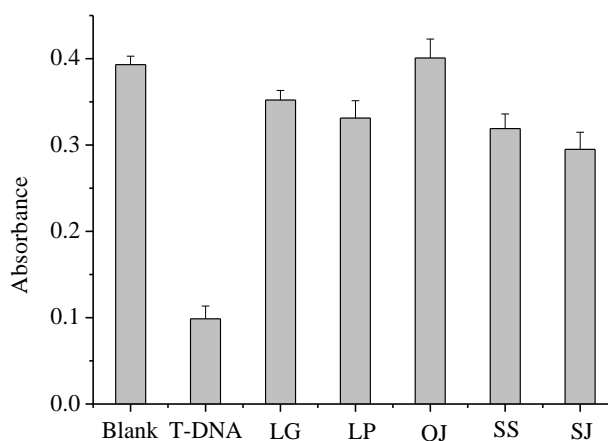
Figure 4. (A) Absorbance spectra of the H_2O_2 mediated ABTS^{2-} colorimetric system with probe-4 ($1.0 \times 10^{-7} \text{ mol L}^{-1}$); T-DNA (a) 1.0×10^{-9} ; (b) 3.0×10^{-9} ; (c) 5.0×10^{-9} ; (d) 8.0×10^{-9} ; (e) 5.0×10^{-8} ; (f) 1.0×10^{-7} and (g) $3.0 \times 10^{-7} \text{ mol L}^{-1}$. Inset: visual color changes of the systems with different concentrations of T-DNA. (B) Absorbance value at 419 nm of the colorimetric system with probe-4 ($1.0 \times 10^{-7} \text{ mol L}^{-1}$) versus T-DNA concentration. Inset: derived calibration curve.



3.6. Specificity Study

To investigate the selectivity of the G-quadruplex DNAzyme MB sensor for PH nrDNA ITS, control experiments were done as follows: nrDNA ITS sequences of the main counterfeit species (C-DNA) in $1.0 \times 10^{-7} \text{ mol L}^{-1}$ were respectively added to the sensor systems, and their absorption signals were collected.

Figure 5. Absorbance value at 419 nm of the G-quadruplex DNAzyme MB colorimetric system containing probe-4 ($1.0 \times 10^{-7} \text{ mol L}^{-1}$) in the presence of T-DNA ($1.0 \times 10^{-7} \text{ mol L}^{-1}$) or C-DNA ($1.0 \times 10^{-7} \text{ mol L}^{-1}$) respectively.



As shown in Figure 5, only the presence of T-DNA makes the absorbance signal decrease largely and there is little decrease in the presence of C-DNA. The above results imply that C-DNA nearly cannot hinder the formation of the intermolecular G-quadruplex DNzyme, and thus has no interference in the detection of T-DNA. We can conclude that the label-free G-quadruplex DNzyme MB sensor can serve as a novel selective oligonucleotide assay for authentication of PH and its adulterants.

4. Conclusions

In the present study, we have combined a novel split mode 1:1:1:1 of G-quadruplex with the MB technique to build a label-free turn-off G-quadruplex DNzyme MB sensor for authentication of PH and its counterfeit species with nrDNA ITS sequence as DNA marker. In the sensor, two probe-4 units shape an intermolecular G-quadruplex DNzyme in the middle possessing high catalytic activity. The presence of T-DNA hinders the formation of the G-quadruplex DNzyme and thus the decrease of catalytic activity revealed by weaker colorimetric and absorbance signals. Through the strategy, the oligonucleotide sensor shows high sensitivity and selectivity toward target T-DNA. To the best of our knowledge, this work provides the first example of development of a G-quadruplex DNzyme MB sensor for discrimination of PH and its counterfeit species. We believe this work may serve as a foundation of further design and utilization of the DNzyme MB sensor for authentication of Traditional Chinese Medicines.

Acknowledgements

Zhenzhu Zheng thankfully acknowledges the support by Bin Qiu, Zhenyu Lin and Guonan Chen (Fujian Provincial Key Laboratory of Analysis and Detection for Food Safety, Fuzhou University) for the CD experiments. The authors are grateful to the Foundation of Social Development, Fujian Provincial Department of Science & Technology (2011Y0034), the Twelve Five “National Science and Technology Support Program” (2011BRI01B06), the Preclinical Studies of the Traditional Chinese Medicine and Quality Control Engineering Technology Research Center Platform of Fujian Province (2009Y2003) and the Independent Research Project of the Fujian Academy of Chinese Medicine (2012fjzyyk-2) for financial support.

References

1. Reinecke, M.G.; Zhao, Y.Y. Phytochemical studies of the Chinese Herb Ta-zi-shen, *Pseudostellaria heterophylla*. *J. Nat. Prod.* **1988**, *51*, 1236–1240.
2. Xu, X.Q.; Li, Q.L.; Yuan, J.D. Determination of three kinds of chloroacetanilide herbicides in *Radix pseudostellariae* by accelerated solvent extraction and gas chromatography-mass spectrometry. *Chin. J. Anal. Chem.* **2007**, *35*, 206–210.
3. Shen, Y.; Han, C.; Liu, J.D.; Liu, A.L.; Ji, X.W.; Liu, C.P. Analysis of volatile components of *Pseudostellaria heterophylla* (Miq.) pax by microwave-assisted solvent extraction and GC-MS. *Chromatographia* **2008**, *68*, 679–682.

4. Lin, H.; Zhao, J.W.; Chen, Q.S.; Zhou, F.; Sun, L. Discrimination of *Radix Pseudostellariae* according to geographical origins using NIR spectroscopy and support vector data description. *Spectrochim. Acta A* **2011**, *79*, 1381–1385.
5. Zhu, Y.; Qin, M.J.; Hang, Y.Y.; Wang, L.Q. Authentication of *Pseudostellaria heterophylla* and its counterfeit species by analysis of rDNA ITS sequences. *Chin. J. Nat. Med.* **2007**, *5*, 211–215.
6. Yip, P.Y.; Chau, C.F.; Mak, C.Y.; Kwan, H.S. DNA methods for identification of Chinese medicinal materials. *Chin. Med.* **2007**, *2*, 1–19.
7. Han, C.; Chen, J.H.; Chen, B.; Lee, F.S.C.; Wang, X.R. Fingerprint chromatogram analysis of *Pseudostellaria heterophylla* (Miq.) Pax root by high performance liquid chromatography. *J. Sep. Sci.* **2006**, *29*, 2197–2202.
8. Han, C.; Shen, Y.; Chen, J.H.; Lee, F.S.C.; Wang, X.R. HPLC fingerprinting and LC-TOF-MS analysis of the extract of *Pseudostellaria heterophylla* (Miq.) Pax root. *J. Chromatogr. B* **2008**, *862*, 125–131.
9. Li, S.H.; Liu, X.H.; Huang, M.H. Analytical studies on HPCE fingerprint of *Radix pseudostellariae*. *Lishizhen Med. Mater. Med. Res.* **2007**, *18*, 820–821.
10. Liu, X.H.; Wang, M.; Cai, B.C.; Wang, Y.X.; Lin, X.Y. GC-MS fingerprint of root tuber of *Pseudostellaria heterophylla*. *Chin. Trad. Herbal Drugs* **2007**, *38*, 113–116.
11. Ruan, G.H.; Li, G.K. The study on the chromatographic fingerprint of *Fructus xanthii* by microwave assisted extraction coupled with GC-MS. *J. Chromatogr. B* **2007**, *850*, 241–248.
12. Wojciechowski, M.F.; Sanderson, M.J.; Baldwin, B.G.; Donoghue, M.J. Monophyly of aneuploid *Astragalus* (Fabaceae): Evidence from nuclear ribosomal DNA internal transcribed spacer sequences. *Am. J. Bot.* **1993**, *80*, 711–722.
13. Baldwin, B.G.; Sanderson, M.J.; Porter, J.M.; Wojciechowski, M.F.; Campbell, C.S.; Donoghue, M.J. The ITS region of nuclear ribosomal DNA: A valuable source of evidence on angiosperm phylogeny. *Ann. Missouri Bot. Gard.* **1995**, *82*, 247–277.
14. Ding, X.Y.; Wang, Z.T.; Xu, H.; Xu, L.S.; Zhou, K.Y. Database establishment of the whole rDNA ITS region of *Dendrobium* species of “fengdou” and authentication by analysis of their sequences. *Acta Pharm. Sin.* **2002**, *37*, 567–573.
15. Ding, P.; Fang, Q. Ribosomal DNA-ITS sequence analysis and molecular identification of *Morinda officinalis* and its counterfeit species. *Chin. Tradit. Herbal Drugs* **2005**, *36*, 908–911.
16. Zhao, Z.L.; Zhou, K.Y.; Dong, H.; Xu, L.S. Characters of nrDNA ITS region sequences of fruits of *Alpinia galanga* and their adulterants. *Planta Med.* **2001**, *67*, 381–383.
17. Bai, D.P.; Brandle, J.; Reeleder, R. Genetic diversity in North American ginseng (*Panax quinquefolius* L.) grown in Ontario detected by RAPD analysis. *Genome* **1997**, *40*, 111–115.
18. Fushimi, H.; Komatsu, K.; Isobe, M.; Namba, T. Application of PCR-RFLP and MASA analyses on 18S ribosomal RNA gene sequence for the identification of three Ginseng drugs. *Biol. Pharm. Bull.* **1997**, *20*, 765–769.
19. Wang, H.T.; Kim, M.K.; Kwon, W.S.; Jin, H.Z.; Liang, Z.Q.; Yang, D.C. Molecular authentication of *Panax ginseng* and ginseng products using robust SNP markers in ribosomal external transcribed spacer region. *J. Pharm. Biomed. Anal.* **2011**, *55*, 972–976.
20. Hon, C.C.; Chow, Y.C.; Zeng, F.Y.; Leung, F.C.C. Genetic authentication of ginseng and other traditional Chinese medicine. *Acta Pharmacol. Sin.* **2003**, *24*, 841–846.

21. Tyagi, S.; Kramer, F.R. Molecular beacons: Probes that fluoresce upon hybridization. *Nat. Biotechnol.* **1996**, *14*, 303–308.
22. Zhang, J.Q.; Wang, Y.S.; Xue, J.H.; He, Y.; Yang, H.X.; Liang, J.; Shi, L.F.; Xiao, X.L. A gold nanoparticles-modified aptamer beacon for urinary adenosine detection based on structure-switching/fluorescence-“turning on” mechanism. *J. Pharm. Biomed. Anal.* **2012**, *70*, 362–368.
23. Yang, R.H.; Jin, J.Y.; Long, L.P.; Wang, Y.X.; Wang, H.; Tan, W.H. Reversible molecular switching of molecular beacon: Controlling DNA hybridization kinetics and thermodynamics using mercury (II) ions. *Chem. Commun.* **2009**, doi:10.1039/B816638B.
24. Bourdoncle, A.; Estevez Torres, A.; Gosse, C.; Lacroix, L.; Vekhoff, P.; Le Saux, T.; Jullien, L.; Mergny, J.L. Quadruplex-based molecular beacons as tunable DNA probes. *J. Am. Chem. Soc.* **2006**, *128*, 11094–11105.
25. Fang, X.H.; Liu, X.J.; Schuster, S.; Tan, W.H. Designing a novel molecular beacon for surface-immobilized DNA hybridization studies. *J. Am. Chem. Soc.* **1999**, *121*, 2921–2922.
26. Zhang, L.B.; Zhu, J.B.; Li, T.; Wang, E.K. Bifunctional colorimetric oligonucleotide probe based on a G-quadruplex DNzyme molecular beacon. *Anal. Chem.* **2011**, *83*, 8871–8876.
27. Travascio, P.; Li, Y.F.; Sen, D. DNA-enhanced peroxidase activity of a DNA aptamer-hemin complex. *Chem. Biol.* **1998**, *5*, 505–517.
28. Fu, L.H.; Li, B.X.; Zhang, Y.F. Label-free fluorescence method for screening G-quadruplex ligands. *Anal. Biochem.* **2012**, *421*, 198–202.
29. Cheng, X.H.; Liu, X.J.; Bing, T.; Cao, Z.H.; Shangguan, D.H. General peroxidase activity of G-quadruplex-hemin complexes and its application in ligand screening. *Biochemistry* **2009**, *48*, 7817–7823.
30. Waller, Z.A.E.; Sewitz, S.A.; Hsu, S.T.D.; Balasubramanian, S. A small molecule that disrupts G-quadruplex DNA structure and enhances gene expression. *J. Am. Chem. Soc.* **2009**, *131*, 12628–12633.
31. Xiao, Y.; Pavlov, V.; Niazov, T.; Dishon, A.; Kotler, M.; Willner, I. Catalytic beacons for the detection of DNA and telomerase activity. *J. Am. Chem. Soc.* **2004**, *126*, 7430–7431.
32. Li, T.; Dong, S.J.; Wang, E.K. Enhanced catalytic DNzyme for label-free colorimetric detection of DNA. *Chem. Commun.* **2007**, 4209–4211.
33. Deng, M.G.; Zhang, D.; Zhou, Y.Y.; Zhou, X. Highly effective colorimetric and visual detection of nucleic acids using an asymmetrically split peroxidase DNzyme. *J. Am. Chem. Soc.* **2008**, *130*, 13095–13102.
34. Nakayama, S.; Sintim, H.O. Colorimetric split G-quadruplex probes for nucleic acid sensing: Improving reconstituted 'DNzyme's catalytic efficiency via probe remodeling. *J. Am. Chem. Soc.* **2009**, *131*, 10320–10333.
35. Fu, R.Z.; Li, T.H.; Lee, S.S.; Park, H.G. DNzyme molecular beacon probes for target-induced signal-amplifying colorimetric detection of nucleic acids. *Anal. Chem.* **2011**, *83*, 494–500.
36. Qiu, B.; Zheng, Z.Z.; Lu, Y.J.; Lin, Z.Y.; Wong, K.Y.; Chen, G.N. G-quadruplex DNzyme as the turn on switch for fluorimetric detection of genetically modified organisms. *Chem. Commun.* **2011**, *47*, 1437–1439.

37. Kolpashchikov, D.M. A binary DNA probe for highly specific nucleic acid recognition. *J. Am. Chem. Soc.* **2006**, *128*, 10625–10628.
38. Shlyahovsky, B.; Li, D.; Katz, E.; Willner, I. Proteins modified with DNazymes or aptamers act as biosensors or biosensor labels. *Biosens. Bioelectron.* **2007**, *22*, 2570–2576.
39. Zhu, D.; Luo, J.J.; Rao, X.Y.; Zhang, J.J.; Cheng, G.F.; He, P.G.; Fang, Y.Z. Utilization of split G-quadruplex makes the design of an assay more flexible. *Anal. Chim. Acta* **2012**, *711*, 91–96.
40. Paramasivan, S.; Rujan, I.; Bolton, P.H. Circular dichroism of quadruplex DNAs: Applications to structure, cation effects and ligand binding. *Methods* **2007**, *43*, 324–331.
41. Rajendran, A.; Nair, B.U. Unprecedented dual binding behaviour of acridine group of dye: A combined experimental and theoretical investigation for the development of anticancer chemotherapeutic agents. *Biochim. Biophys. Acta* **2006**, *1760*, 1794–1801.

© 2013 by the authors; licensee MDPI, Basel, Switzerland. This article is an open access article distributed under the terms and conditions of the Creative Commons Attribution license (<http://creativecommons.org/licenses/by/3.0/>).